

## Modeling and optimization of quality parameters in EDM of Nimonic 90 using Evolutionary Techniques

M.Jawahar<sup>1</sup>, Ch.Sridhar Reddy<sup>2</sup>, Ch.Srinivas<sup>3</sup>

<sup>1</sup>Research Scholar, Department of Mechanical Engineering, JNTUH, Kukatpally, Hyderabad, -Telangana, India.

<sup>2</sup>Professor, Department of Mechanical Engineering, JNTUH-CEM, Telangana.

<sup>3</sup> Professor, Department of Mechanical Engineering, Vaageswari College of Engineering, Karimnagar, Telangana, India  
jawahar.mamidalal23@gmail.com

### Abstract

Nickel superalloy is a material that belongs to the advanced category and is frequently used in a number of significant industries, including those of aerospace, automobiles, and missiles because of its exceptional mechanical, physical, and chemical qualities, it is used in a variety of applications. Such unique materials may now be machined due to the development of complex machining processes. Nowadays, one common AMP for machining nickel alloys is electrical discharge machining. Discharge current ( $I_p$ ), pulse-on time ( $T_{on}$ ), pulse-off time ( $T_{off}$ ) and nano powder concentration were tested as process parameters in the present research work using EDM on a Nimonic 90. Surface roughness has been taken into consideration as an output parameter together with the rate of material removal and tool wear. Both the quality parameters and RSM have been developed. Single objective optimization of the quality parameters was then carried out using a TLBO and PSO approach in the RSM. It has been noted that TLBO produces superior outcomes to PSO.

**Key words:** MRR, SR, TWR, TLBO, PSO, RSM, Nimonic 90.

### 1. Introduction

EDM is a non-conventional electro-thermal machining process. Spark eroding, sometimes known as spark machining, is a type of machining that uses sparks. It's frequently used for machining hard, high-demand materials like titanium, superior hardened super alloy combinations, and other industrial applications. [1, 2]. According to a review of the literature, NPMEDM is a viable approach for resolving the limits of regular EDM machining methods. Despite substantial research in the field of powdered mixed EDM using various powders such as Titanium, Silicon, Graphite, and so on, it was found that NPMEDM was invented in the earlier centuries. One of the most essential and novel ways for overcoming EDM method constraints and expanding the EDM limit [3]. The use of nanoparticles such as aluminium powder and multiwalled carbon nanotube (CNT) powder into dielectric fluid has enhanced the MRR, TWR, and surface roughness of machined components (SR). A unique method known as nano powder mixed EDM is utilised to remove the found defects. The insulating strength of the dielectric is reduced when it is linked with powder, the process becomes more stable, and the spark gap between the tool material and the work material increases. MRR and SR will be high if the discharge parameters are optimized [4]. The effect of adding carbon nanotubes into the oil flux dielectric during the Ti-6Al-4V EDM process was examined by Shabgard and Khobragade et al. In this experiment, copper was employed as a tool. When carbon nanotubes were combined with dielectric, surface micro cracks were reduced. It was also discovered that combining CNT particles reduced MRR, TWR, and SR [5]. Kumar et al. studied the EDM technique's performance when cutting Inconel 825 with an  $Al_2O_3$  nano particles blended dielectric. MRR and surface roughness improved considerably when nano particles were introduced to the shown water dielectric fluid. Machining tools made of copper were utilised. They discovered that low-cost  $Al_2O_3$  powder may be employed in industrial applications successfully [6].

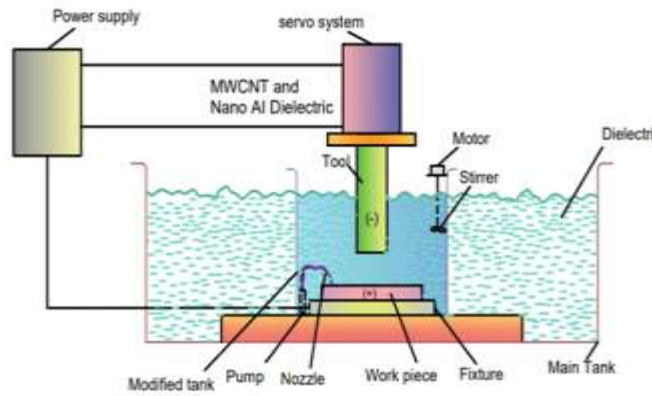


Figure.1 working model of NPMEDM

An extensive review of the literature demonstrates that a lot of research has been done to determine the effects of various input control elements on different quality measures. To forecast process behavior, researchers have created a variety of traditional and AI-based models. Additionally, using traditional optimization techniques, researchers have attempted to optimize the process behavior to produce the optimum results. However, during EDM of Nimonic 90, researchers seldom ever employed evolutionary optimization techniques as TLBO, differential evolution, or PSO. With the aforementioned research gap in mind, Nimonic 90 has undergone EDM using various peak current, pulse-on and pulse-off times, and powder concentration. The three most crucial performance variables, MRR, SR, and TWR, have been assessed. The quality parameters have been created for the RSM. Furthermore, utilizing TLBO and PSO, single objective optimization of MRR, SR, and TWR was carried out using the created RSM model as the objective function. Finally, the MRR, SR, and TWR performance of TLBO and PSO have been compared.

## 2.Experimental Details

In this study, the powder concentrations of CNTs, nano Al, and a mixture of nano aluminium and CNTs in the dielectric medium were varied. The study's work material was Nimonic 90 nickel super alloy, which was cut into a  $70 \times 35 \times 4 \text{ mm}^3$  size utilizing a wire cut EDM process. The composition of Nimonic 90 nickel alloy is shown in Table 1. Table 2 shows the parameters of a copper tungsten tool with a 14 mm diameter and a length of 60 mm used in the studies.

Table 1. Nimonic 90's chemical composition

Components	Al	B	C	Co	Cr	Cu	Fe	Mn	Pb	S	Si	Ti	Zr	Ni	
Wt (%)	Max	2	0.02	0.13	21	21	0.2	2	1	0.0025	0.015	1	3	0.15	Bal
	Min	1			15	18						2			

The electrode was manufactured of copper-tungsten and had a cross-section of 14mm x 60mm. Copper-tungsten was chosen because it has a high conductivity and a high melting point. Because EDM is a thermal process, the high electrical conductivity of the electrode attracts more electrons, and the electrode's high melting point results in a low wear ratio.

Table 2 Characteristics of copper-tungsten.

Material	Melting Point(°C)	Density(g/cm <sup>3</sup> )	Young Modulus(N/mm <sup>2</sup> )	Hardness (HV)	Thermal Conductivity(W/mK)	Electrical Resistivity× (10 <sup>-7</sup> Ωm)
W70Cu30	3410	14.3	225×10 <sup>3</sup>	175	154	7.27

Table 3 lists the input parameters that were examined, as well as their levels. The tests were carried out using L<sub>27</sub> OA.

Table 3 Selection of levels for factors

Factors with Symbol and units	Levels		
	Level 1	Level2	Level3
MWCNT powder concentration	0.5	0.75	1
Nano Al powder concentration	2.0	2.50	3.0
Dischargecurrent	5	10	15
Pulse-on-time	25	50	75
Pulse-off-time	12	24	36

Table 4 Experimental observation

Run No	Process parameters					Response parameters		
	CNTs powder	Al powder	I <sub>p</sub>	T <sub>on</sub>	T <sub>off</sub>	MRR (mm <sup>3</sup> /min)	SR (μ)	TWR (mm <sup>3</sup> /min)
1.	0.50	2.0	5	25	12	20.502	2.289	0.141
2.	0.50	2.0	10	50	24	18.924	1.836	0.201
3.	0.50	2.0	15	75	36	18.477	2.486	0.121
4.	0.50	2.5	5	50	36	17.756	2.963	0.217
5.	0.50	2.5	10	75	12	16.176	2.709	0.257
6.	0.50	2.5	15	25	24	15.722	3.559	0.197
7.	0.50	3.0	5	75	24	13.182	3.372	0.268
8.	0.50	3.0	10	25	36	12.605	2.719	0.307
9.	0.50	3.0	15	50	12	12.152	3.569	0.247
10.	0.75	2.0	5	25	12	27.938	3.524	0.255
11.	0.75	2.0	10	50	24	26.352	3.071	0.314
12.	0.75	2.0	15	75	36	25.901	3.521	0.235
13.	0.75	2.5	5	50	36	25.187	3.998	0.331
14.	0.75	2.5	10	75	12	23.602	3.645	0.371
15.	0.75	2.5	15	25	24	23.154	4.495	0.311
16.	0.75	3.0	5	75	24	18.618	4.607	0.382
17.	0.75	3.0	10	25	36	17.032	4.154	0.421
18.	0.75	3.0	15	50	12	17.583	5.014	0.361
19.	1.00	2.0	5	25	12	32.788	5.350	0.327
20.	1.00	2.0	10	50	24	31.2076	4.896	0.387
21.	1.00	2.0	15	75	36	30.767	5.346	0.307
22.	1.00	2.5	5	50	36	30.044	5.923	0.403
23.	1.00	2.5	10	75	12	28.465	5.570	0.453
24.	1.00	2.5	15	25	24	28.012	6.220	0.383
25.	1.00	3.0	5	75	24	24.465	6.433	0.454
26.	1.00	3.0	10	25	36	22.887	5.879	0.513
27.	1.00	3.0	15	50	12	21.445	6.129	0.433

### 3. Modeling and optimization

#### 3.1 Response surface method (RSM)

When several variables influence a desire response, regression structural modelling is the most effective statistical and mathematical tool for modelling and analysis (RSM). The goals are to build a relationship between the independent factors and the desire response, as well as to connect the desire response to the supplied variables [9]. A mathematical model has been used to show a connection between the independent factors and the desire response ( $Z_u$ ). A reasonable approximation relationship is found when there is no known relationship between two variables. In the situation that the relationship is not linear, Eq. (3) constructs and describes the second order model as follows:

$$Z_u = \beta_0 + \sum_{i=1}^k \beta_i Y_i + \sum_{i=1}^k \beta_{ii} Y_i^2 + \sum_i \sum_j \beta_{ij} Y_i Y_j \dots \dots \dots (1)$$

$Y_i$  stands for input variables,  $Y_i^2$  &  $Y_i Y_j$  are squares and interaction terms of these provided input process variables, and  $Z_u$  represents the related response, such as MRR, SR, and TWR in the current study. Using RSM, the quadric model is created to determine how responses (MRR, SR, and TWR) interact with process factors [16,17]. Minitab 19 is used to do the analysis.

#### 3.2 Optimization

The hybrid RSM-TLBO and RSM-PSO methods were employed for both modelling and process optimization. In this case, the optimization problem's objective function is as follows:

Find  $x_1, x_2, x_3, x_4$  and  $x_5$

Maximize

$$\text{MRR} = -17.17 + 53.45 x_1 + 20.91 x_2 - 0.501 x_3 - 0.0033 x_4 - 0.0583 x_5 - 13.47 x_1^2 - 5.20 x_2^2 + 0.0204 x_3^3 - 0.000090 x_4^2 + 0.00078 x_5^2 - 4.00 x_1 * x_2 - 0.132 x_1 * x_3 + 0.0134 x_1 * x_4 + 0.0276 x_1 * x_5 \quad \text{E. q (2)}$$

Minimize

$$\text{SR} = -4.79 - 0.35 x_1 + 5.57 x_2 - 0.3664 x_3 - 0.0097 x_4 + 0.0264 x_5 + 4.613 x_1^2 - 0.882 x_2^2 + 0.02187 x_3^2 + 0.000096 x_4^2 - 0.000845 x_5^2 - 0.133 x_1 * x_2 - 0.0667 x_1 * x_3 - 0.00133 x_1 * x_4 + 0.0138 x_1 * x_5 \quad \text{E. q (3)}$$

Minimize

$$\text{TWR} = -0.8505 + 0.8067 x_1 + 0.3031 x_2 + 0.04574 x_3 + 0.000840 x_4 + 0.001579 x_5 - 0.3076 x_1^2 - 0.03822 x_2^2 - 0.002389 x_3^2 - 0.000008 x_4^2 - 0.000036 x_5^2 + 0.01333 x_1 * x_2 + 0.000000 x_1 * x_3 - 0.000133 x_1 * x_4 + 0.000278 x_1 * x_5 \quad \text{E. q (4)}$$

With the range of process input parameters

$$0.5 \leq X_1 \leq 1$$

$$2 \leq X_2 \leq 3$$

$$5 \leq X_3 \leq 15$$

$$25 \leq X_4 \leq 75$$

$$12 \leq X_5 \leq 36$$

The hybrid RSM-TLBO and RSM-PSO algorithm has been implemented using the Matlab R2016a software.

#### 3.3 Teaching Learning-based Optimization (TLBO)

TLBO which is computationally simpler than genetic algorithms (GA), particle swarm optimization (PSO), and other methods, was recently developed by Rao et al. TLBO updates the population of solutions in two stages, replicating classroom activity by learning first from the teacher and then from

one another. Rao et al. (13-15) employed the PSO technique to optimize MRR, dimensional accuracy, and tool life in the electrochemical machining process while giving equal weight to all responses.

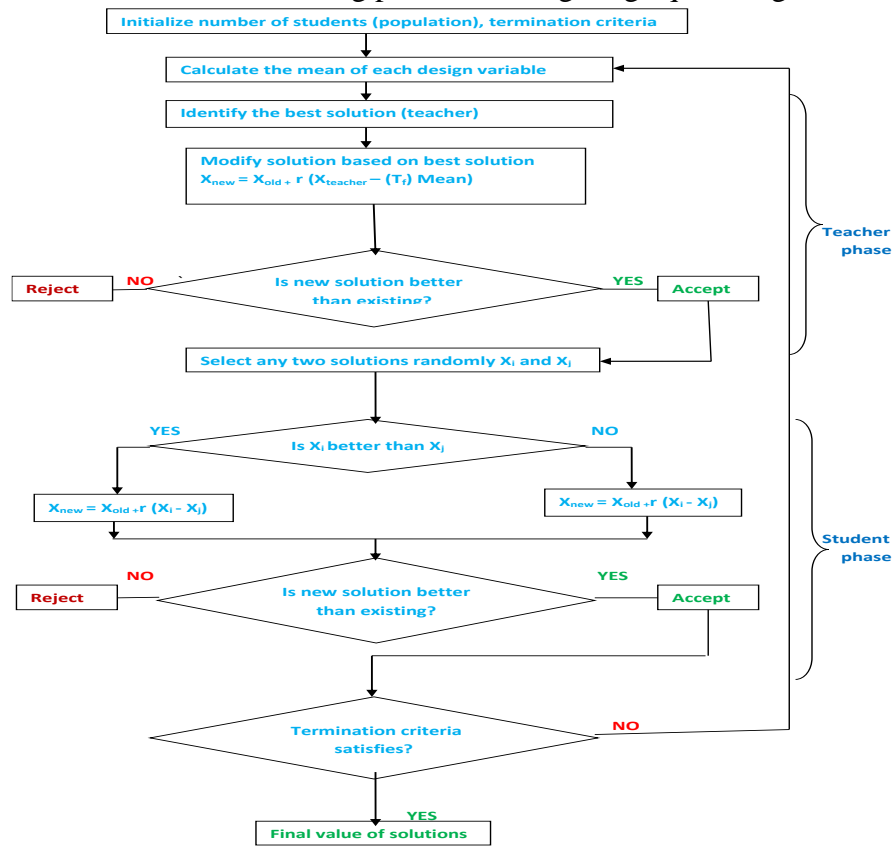


Figure 2: Flowchart of TLBO Algorithm

Experimental data and mathematical modelling were used to establish the optimization performance of TLBO. Here, replies were optimized with a single purpose. For the parametric optimization in the EDM process, a computer code was created using MATLAB R2016a while taking into account the following factors: population size = 50 and numbers of generations = 500

Table 5: Inputprocess Parameters for Matlab code

Design Parameters= 5	Population Size =50	Maximum Iterations=500
Lower bounds= [0.5 2 5 25 12]	Upper bounds= [0.5 315 75 36]	

### 3.4 Particle Swarm Optimization (PSO)

Kennedy and Eberhart invented the population-based evolutionary computation technique known as the particle swarm optimization (PSO) algorithm in 1995 [7], inspired by the social behavior of fish schooling and bird flocking. Each member of its population is referred to as a particle, and the population as a swarm [8]. Each particle scans the solution space in order to identify the global optimal solution. Each participant in PSO is referred to as a particle, and each particle moves around the search region at a velocity that is constantly updated by the contribution of each individual particle as well as the contribution of neighboring particles or the contribution of the entire swarm. Members of the entire population are kept around during the search process to allow knowledge to be socially shared and the

search to be directed toward the best location in the search space. Based on the global neighborhood, each particle advances toward its best previous location as well as the best particle in the entire swarm, known as the gbest. Each particle progresses toward its best prior location and toward the best particle in its limited region based on the local variation known as the pbest model. PSO is generally stated as a simple, well-balanced mechanism capable of progressing and changing in response to both local and global exploration capacities. Unlike evolutionary algorithms, all particles have a tendency to quickly converge to the optimal solution, even in the local form. Job scheduling, power and voltage management problems, and other domains have profited from the use of SO due to its simple idea, simple implementation, and speedy convergence [10]. PSO's initial population and settings are generated at random. After evaluating the fitness function, the PSO algorithm iteratively executes the following steps:

- Personal best, or each person's prior best value, is altered if a greater value is discovered.
- Then, utilizing the most recent adjustments to their velocities, which are based on individual and collective best performance, each particle's locations are modified's. (8) and (9) are used to update each particle's position and velocity after determining the individual and overall best values.

$$v_{ij}^t = w^{t-1} v_{ij}^{t-1} + c_1 r_1 (p_{ij}^{t-1} - x_{ij}^{t-1}) + c_2 r_2 (g_{ij}^{t-1} - x_{ij}^{t-1}) \quad \text{Eq. (5)}$$

$$x_{ij}^t = x_{ij}^{t-1} + v_{ij}^t \quad \text{Eq. (6)}$$

where  $v_{ij}^t$  represents the velocity of particle  $i$  in relation to the  $j$ th dimension ( $j = 1, 2, \dots, n$ ) at iteration  $t$ .  $p_{ij}$  represents the position value of the  $i$ th personal best in regard to the  $j$ th dimension.  $g_{ij}$  represents the global best (g best), or the best of the p best among all particles. The value of  $x_{ij}^t$  represents the position of the  $i$ th particle in reference to the  $j$ th dimension. The cognitive and social factors are both positive acceleration characteristics that provide the ideal balance of exploration and exploitation.  $r_1$  and  $r_2$  are random numbers that provide the particle velocities a stochastic component in order to imitate flock behavior. The inertia weight parameter  $w$  governs the effect of earlier velocities on the current velocity of each particle. The parameter  $w$  thereby balances the swarm's ability to explore both locally and globally. The suggested value for the inertia weight,  $w$ , is to start with a high number to optimize the global search of the search space and then decrease it to acquire more accurate solutions, allowing local search in the latter stages. In most cases, the inertia weight is determined by

$$w = w_{max} - \frac{w_{max} - w_{min}}{iter_{max}} \quad \text{Eq. (7)}$$

where  $iter_{max}$  is the maximum number of iterations,  $iter$  is the current iteration number, and  $w_{min}$  and  $w_{max}$  are the starting and ultimate weights.

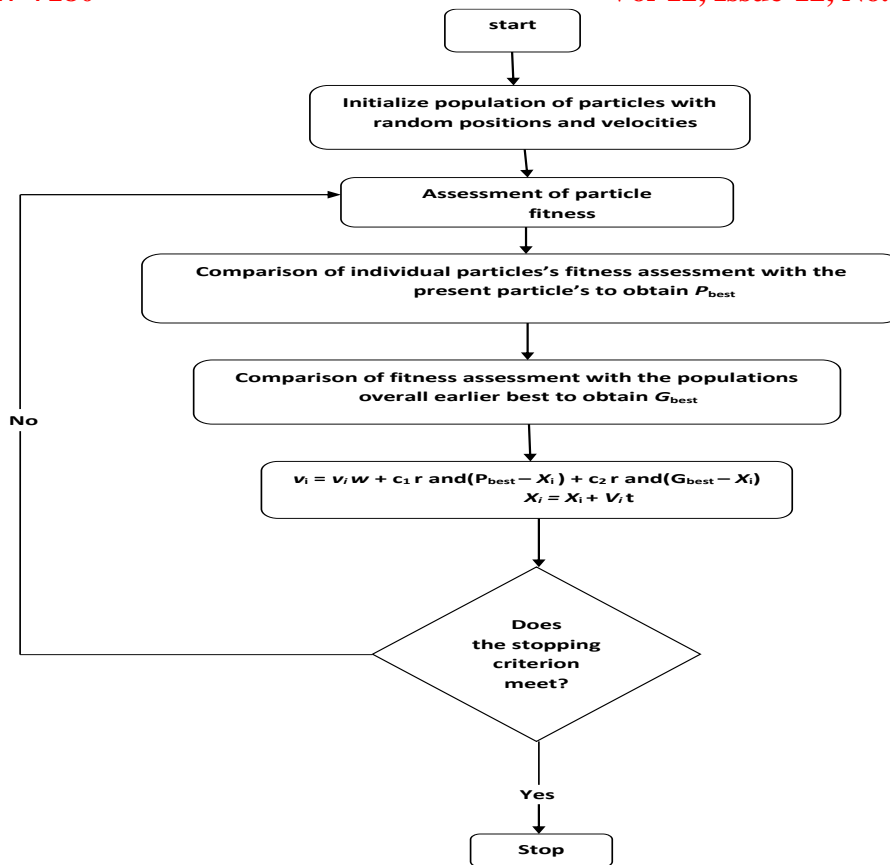


Figure 3: Flow chart of PSO Algorithm

#### 4.Result and Discussion

Table 4 depicts the Taguchi  $L_{27}$ OA and the performance measures based on the results. ANOVA is used on performance measures such as material removal rate, tool wear rate, and surface roughness to investigate the impact of major process parameters. Minitab 19 was used to analyse the experimental data. For the regression models, a quadratic model is produced for each of the three responses separately. Once the superfluous terms are removed, the final equation for MRR in coded units is as follows.

$$\begin{aligned}
 \text{MRR} = & -17.17 + 53.45 x_1 + 20.91 x_2 - 0.501 x_3 - 0.0033 x_4 - 0.0583 x_5 - 13.47 x_1^2 - 5.20 x_2^2 + 0.0204 x_3^3 - 0.000090 x_4^2 + \\
 & 0.00078 x_5^2 - 4.00 x_1 * x_2 - 0.132 x_1 * x_3 + 0.0134 x_1 * x_4 + 0.0276 x_1 * x_5
 \end{aligned}
 \tag{8}$$

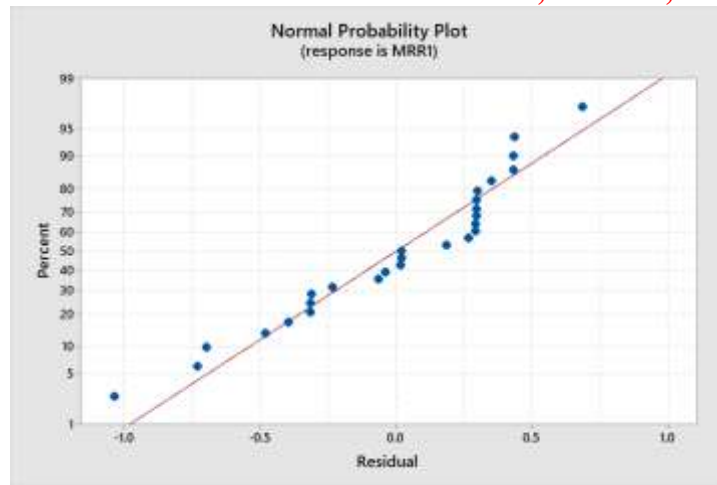


Figure 4. Normal Probability Plot for Surface Roughness

The F-values are used to find the significance check. The P-value indicates the likelihood that noise will cause the F-value to be higher than the computed value. If a term's P-value, or 95% confidence level, is less than 0.05, its significance is determined. Since the lack of fit has been established, the P-value is higher than 0.05. It means that the model is constructed without the irrelevant element, and as a result, the model fits very well. The table makes it obvious that the developed model is an important one. For MRR, the  $R^2$  and Adj.  $R^2$  coefficient of determination values were discovered to be 0.9951 and 0.9894, respectively. This implies that the regression model provides the most thorough account of the relationship between the factors and the response (MRR). TWR and Ra showed similar results, with coefficients of determination ( $R^2$ ) and adj.  $R^2$  values of 0.9942 and 0.9878, respectively. According to the normal probability plot for MRR given in Fig. 3, the residuals have a normal distribution, which suggests that the errors are regularly distributed along a straight line. The residuals in Figure 5's normal plot for TWR are regularly distributed along the line. The equation (6) below is tributed down the straight line to provide the second order regression equation for TWR.

$$\text{TWR} = -0.8505 + 0.8067 x_1 + 0.3031x_2 + 0.04574x_3 + 0.000840 x_4 + 0.001579 x_5 - 0.3076 x_1^2 - 0.03822 x_2^2 - 0.002389 x_3^2 - 0.000008 x_4^2 - 0.000036 x_5^2 + 0.01333 x_1 * x_2 + 0.000000 x_1 * x_3 - 0.000133 x_1 * x_4 + 0.000278 x_1 * x_5 \quad \text{E. q (6)}$$

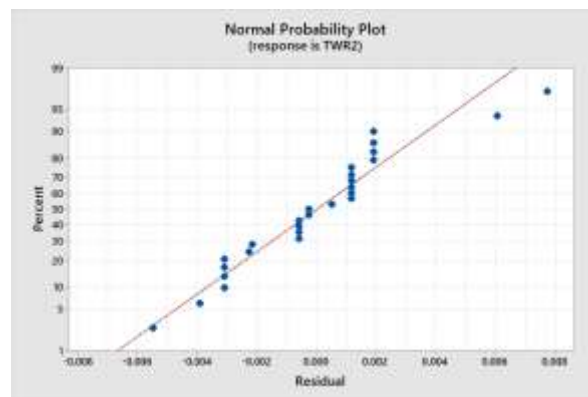


Figure 5. Normal Probability Plot for TWR

Similar to how  $R_a$  is clearly depicted in Fig. 6, the distribution of the residual is uniform along the line of the normal distribution. The impact of low voltage current and pulse on time on surface roughness is depicted in Fig. 8. Where it is discovered that  $R_a$  is tiny at high flushing pressure. The following gives the second order model equation for  $R_a$ :

$$SR = -4.79 - 0.35 x_1 + 5.57x_2 - 0.3664 x_3 - 0.0097x_4 + 0.0264 x_5 + 4.613x_1^2 - 0.882 x_2^2 + 0.02187 x_3^2 + 0.000096 x_4^2 - 0.000845 x_5^2 - 0.133 x_1*x_2 - 0.0667 x_1*x_3 - 0.00133 x_1*x_4 + 0.0138 x_1*x_5 \quad \text{E. q (10)}$$

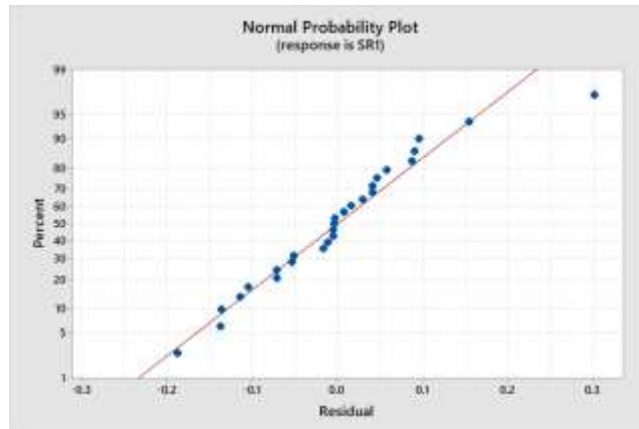


Figure 6. Normal Probability Plot for Surface Roughness

Table 6: Confirmatory test result for MRR, SR and TWR

Algorithm	Response value obtained from TLBO algorithm			Response value obtained from PSO algorithm			Experimental value		
	MRR	SR	TWR	MRR	SR	TWR	MRR	SR	TWR
Optimum value	23.130	2.491	0.193	22.567	2.1256	0.179	21.345	2.156	0.766

Table 6 displays the results of the confirmatory tests conducted using both methods, together with the ideal parametric setting and the calculated value of the overall utility index. With errors of 10.2% and 9.8% for TLBO and PSO, respectively, the computed values of the overall utility index for the confirmatory test are determined to be 6.31 and 5.98. The outcomes of the PSO algorithm are more advantageous for achieving increased machining efficiency, as is seen from the table.

### Conclusions

The TLBO and PSO algorithms were used in this study to perform single-objective optimization of the MRR, SR, and TWR for the Nimonic 90 NPMEDM process. The optimal MRR, SR, and TWR values were determined. The single objective optimization method can be used to meet the specific needs of the manufacturing unit. For example, if MRR is important in the production of goods, the producer can strive to maximize MRR value. As a result, the TLBO algorithm proved to be a low-cost solution for determining the optimal values of input process parameters.

### References

1. Pawan, K, Meenu, G, and Vineet, K. "Surface Integrity Study of Inconel 825 Super Alloy WEDMed Specimen." International Journal of Data Network Science, 2018, 77–88.

2. Sunil Sheshrao Baraskar, S.S Banwait, and S.C. Laroia. "Multiobjective Optimization of Electrical Discharge Machining Process Using a Hybrid Method." *Materials and Manufacturing Processes*, 4, March 2013, 348–54. doi.org/10.1080/10426914.2012.700152.
3. Rafa, S, Dorota, O.S, and Tomasz, C. "Multi-Response Optimization of Electrical Discharge Machining with the Desirability Function Micro Machines." *Micro Machines* 10, no. 72 (2019).
4. M. Jawahar, Ch. Sridhar Reddy, and Ch. Srinivas. "A Review of Performance Optimization and Current Research in PMEDM." *Today: Proceedings* 19, no. 2 (August 2019): 742–47. <https://doi.org/doi.org/10.1016/j.matpr.201908.122>.
5. H.K. Kansal, S. Singh and P. Kumar. (2007), "Technology and research advancements in powder mixed electric discharge machining (PMEDM)," *Journal of Materials Processing Technology*, 184, pp. 32–41.
6. S. Tripathy and D.K. Tripathy. (2016), "Multi-attribute optimization of machining process parameters in powder mixed electro-discharge machining using TOPSIS and grey relational analysis," *Engineering Science and Technology*, Vol. 19/1, pp. 62–70.
7. Kennedy, J and R. Eberhart . (1995), "Particle swarm optimization" (Perth, Australia), *Proceedings IEEE, International Conference on Neural Network (ICNN-95)*, Vol. 4, pp. 1942–1948.
8. Wu, Q.H, He S and Prempain, E. (2004), "An improved particle swarm optimization for mechanical design optimization problems," *Engineering Optimization*, Vol. 5/36, pp. 585–605.
9. D.C. Montgomery. (2001), "Design & Analysis of Experiments," *Wiley, New York*.
10. M.R. Singh, S.S. Mahapatra, A swarm optimization approach for flexible flowshop scheduling with multiprocessor tasks, *Int. J. Adv. Manuf. Technol.* 62 (1)(2012) 267–277.
11. H. Yoshida, K. Kawata, Y. Fukuyama, S. Takayama, Y. Nakanishi, A particleswarm optimization for reactive power and voltage control considering voltage security assessment, *IEEE Trans. Power Syst.* 15 (4) (2000) 1232–1239.
12. Rao, R. V.; Savsani, V. J.; Vakharia, D. P. Teaching–learning-based Optimization: A Novel Method for Constrained Mechanical Design Optimization Problems. *Comput. Aided Des.* 2011, 43(3),303–315. DOI: 10.1016/j.cad.2010.12.015.
13. Rao, R. V.; Pawar, P. J.; Shankar, R. Multi-objective Optimization of Electrochemical Machining Process Parameters Using a Particle Swarm Optimization Algorithm. *Proc. Inst. Mech. Eng. Part B J. Eng. Manuf.* 2008, 222(8), 949–958. DOI: 10.1243/09544054JEM1158.
14. Rao, R. V.; Rai, D. P.; Balic, J. Multi-objective Optimization of Machining and Micro-machining Processes Using Non-Dominated Sorting Teaching–learning-based Optimization Algorithm. *J. Intell. Manuf.* 2016. DOI: 10.1007/s10845-016-1210-5.
15. Maity, K.; Mishra, H. ANN Modelling and Elitist Teaching Learning Approach for Multi-objective Optimization of  $\mu$ -EDM. *J. Intell. Manuf.* 2016. DOI: 10.1007/s10845-016-1193-2.
16. Sen, R.; Choudhuri, B.; Barma, J. D.; Chakraborti, P. Optimization of Wire EDM Parameters Using Teaching Learning Based Algorithm during Machining of Maraging Steel 300. *Mater.Today Proc.* 2018, 5(2), 7541–7551. DOI: 10.1016/j.matpr.2017.11.426.